Bayesian parameter calibration of a one-dimensional hemodynamic model

Diovana de Oliveira Mussolin[1], Luis Alonso Mansilla Alvarez[1], Pablo Javier Blanco[1]

[1]*Laboratório Nacional de Computação Científica - LNCC*
Avenida Getúlio Vargas 333, 25651-075, Petrópolis-RJ, Brasil
diovanam@posgrad.lncc.br, lalvarez@lncc.br, pjblanco@lncc.br

Abstract. In this work, we couple a Bayesian optimization approach with a one-dimensional blood-flow model of the arterial system (known as ADAN86) to achieve a flexible and efficient strategy for calibrating model parameters when flow/pressure waveform data is available. The optimization is addressed in the frequency domain by minimizing the discrepancies between the major features of the model-predicted and measured waveforms. The proposed optimization strategy is validated in two synthetic scenarios, testing their capabilities in the calibration of physiological parameters such as elastic modulus, viscoelasticity of arterial wall, and luminal radius, among others. Obtained results show a good compromise between the accuracy of the predictions and the number of iterations performed in the optimization process.

Keywords: Bayesian optimization, model calibration, computational hemodynamics.

1 Introduction

The understanding of the onset and progression of several cardiovascular diseases presents a significant challenge in healthcare due to their direct impact as the most prevalent cause of death worldwide. Computational hemodynamics has emerged as an efficient and non-invasive tool, capable of providing physiological insights and important blood-related indexes useful in the medical practice [1–3]. In this context, the ADAN86 model, a one-dimensional model of the cardiovascular system [4, 5], plays a crucial role in describing blood flow phenomena at the systemic circulation scale. However, a patient-specific approach requires calibration and adjustment of model parameters to reflect the circulatory state of individual patients.

In the field of parameter optimization, Bayesian optimization is a particularly advantageous approach for complex scenarios, when the dimension of the parameter space is high or when the function to be optimized possesses multiple local maxima. [1, 6, 7]. Based on the definition of a surrogate function to represent the probable improvement in the prediction, the Bayesian process sequentially tests new parameter points, which implies the solution of the blood flow model, converging (when convergence is achieved) to the best parameter combination that reduces the mismatch between prediction and measure.

This work explores the potentialities of the coupling of the Bayesian optimization approach and the one-dimensional blood flow model for parameter identification. As in the hemodynamic model, each parameter is defined with a reference value, the approach taken here is based on the use of a multiplicative factor that alters the parameter value along the optimization process. Thus, the goal is to estimate some of the parameters of the ADAN86 blood flow model using Bayesian optimization such that the model predictions match with synthetically-generated patient data, i.e., with virtual patient data generated by the same ADAN86 model. This study illustrates the effectiveness of Bayesian optimization in personalizing complex physiological models, demonstrating its potential to adjust models to reflect the individual characteristics of each patient.

2 Methodology

2.1 Blood flow model

The ADAN (Anatomically Detailed Arterial Network) model, developed according to medical literature, provides a comprehensive representation of the human arterial system, enabling accurate computational simulations in

the field of computational hemodynamics [8, 9]. This model provides a one-dimensional description of the blood flow dynamics whose governing equations are:

$$\begin{aligned} \frac{\partial A}{\partial t} + \frac{\partial Q}{\partial x} &= 0 \\ \frac{\partial Q}{\partial t} + \frac{\partial}{\partial x}\left(\alpha \frac{Q^2}{A}\right) + \frac{A}{\rho}\frac{\partial P}{\partial x} &= \frac{8\pi\mu}{\rho A} Q, \end{aligned} \tag{1}$$

where A is the cross-sectional area of the lumen, Q is the flow rate, P is the mean blood pressure over the cross-sectional area, ρ is the blood density, μ the viscosity of the fluid and α the momentum correction factor. Additionally, a constitutive equation relating the pressure and the strains in the arterial wall is required. The proposed equation accounts for the behavior of the elastin and collagen fibers as well as for the smooth muscle contribution, and reads:

$$P = P_0 + \frac{\pi h R_0}{A}\left[E_e \varepsilon + E_c \epsilon_r ln(e^u + 1) + \gamma \dot{\varepsilon}\right], \tag{2}$$

where $\varepsilon = \sqrt{\frac{A}{A_0}} - 1$ (with $\dot{\varepsilon} = \frac{\dot{A}}{2\sqrt{A A_0}}$) and $u = \frac{\varepsilon - \varepsilon_0}{\epsilon_r}$. Let r be the radius of the lumen, $A = \pi r^2$ (correspondingly A_0 is the reference lumen area at the pressure $P_0 = 1 \times 10^5$ dyn/cm^2, which is of the order of diastolic pressure). Here, h is the wall thickness, E_e is the elastic modulus of elastin, E_c is the elastic modulus of collagen fibers (ϵ_r and ε_0 characterize fiber recruitment distribution), and γ is the effective viscoelastic parameter.

The ADAN model has been used in various research applications in computational hemodynamics [10, 11], but it poses a challenge due to the computational cost that results from the extreme anatomical detail of the network. To reduce the computational costs, a simplified version, named ADAN86, was proposed by including the most relevant arterial vessels while delivering reasonable results when compared to the ADAN model, especially in the primary arteries [5]. Using the same one-dimensional equations of mass conservation and linear momentum conservation as described in 1, along with the constitutive behavior of the arterial wall 2. The terminal arterial segments in both ADAN and ADAN86 are modeled as Windkessel elements, allowing these models to capture important hemodynamic characteristics of the relation between peripheral pressure and flow rate [5].

2.2 Bayesian optimization

Bayesian optimization (BO) is a technique aimed at identifying the optimal set of parameters to reach the extrema of a black-box function [12]. Roughly speaking, Bayesian Optimization is based on the construction of a posterior distribution of functions, known as the Gaussian Process (GP), which is a probabilistic model used to represent the uncertainty about the function we wish to optimize [13]. This Gaussian process is characterized by a mean function $m(\boldsymbol{x})$, representing the best estimate of the (unknown) cost function, and a covariance function $k(\boldsymbol{x}, \boldsymbol{x}')$, which represents the uncertainty on the prediction. We define these two functions for a real process $f(\boldsymbol{x})$ as follows:

$$m(\boldsymbol{x}) = \mathbb{E}[f(\boldsymbol{x})] \tag{3}$$

$$k(\boldsymbol{x}, \boldsymbol{x}') = \mathbb{E}[(f(\boldsymbol{x}) - m(\boldsymbol{x}))(f(\boldsymbol{x}') - m(\boldsymbol{x}'))], \tag{4}$$

the GP is described as

$$f(\boldsymbol{x}) \sim \mathcal{GP}(m(\boldsymbol{x}), k(\boldsymbol{x}, \boldsymbol{x}')), \tag{5}$$

with the function k commonly referred to as the kernel of the GP. The selection of an appropriate kernel is based on smoothness assumptions on the function. Given an initial set of points and the corresponding function evaluations, a GP can be constructed as a non-parametric approximation of the true function f. Hence, the GP is updated as more information (evaluations) of the (unknown) black-box function is available, resulting in an iterative process: suggest a point $\boldsymbol{x}$, evaluate the black-box function f, and update the mean/covariance. To guide the selection stage, rather than a purely random search or a grid-based search, the GP is combined with the so-called acquisition functions, which is a surrogate description of the prediction uncertainty. Thus, the acquisition function is used for determining the better sampling point to be tested in order to maximize the improvement. Among several options available, the most commonly used ones are Upper Confidence Bound (UCB), Probability of Improvement (PoI),

and Expected Improvement (EI) [12, 14]. The choice depends on the problem and the desired behavior in exploring the search space and the nature of model uncertainties.

The Probability of Improvement (PoI) prioritizes the exploration of regions with a high likelihood of surpassing the best-known outcome. It evaluates the probability that the function at a new point will exceed the best-observed value by a specific threshold. The Upper Confidence Bound (UCB) selects the next evaluation point based on an upper confidence limit, which represents the uncertainty associated with the estimate of the cost function. This is calculated using the predictive mean of the GP, along with an exploration term that balances the trade-off between exploring new regions and exploiting promising areas. In contrast, the Expected Improvement (EI) aims to identify the next evaluation point that has the maximum potential to improve the best-observed value. The EI takes into account the difference between the model's prediction for a point and the best-observed value to date [12].

2.3 Cost function

In the BO process, the cost function (F_c) is crucial as it quantifies the discrepancies between the model predictions and the patient's actual data. In this study, we focus on the flow and pressure waveforms in different districts within the cardiovascular system, analyzing them exclusively in the frequency domain. This approach allows us to circumvent issues such as time lag and lack of synchronization in signal acquisition, as well as to filter out noise and high-frequency disturbances.

The cost function is defined by considering N harmonic components of the curves predicted by the ADAN86 model and the patient's actual measurements. This is expressed as follows:

$$\varepsilon_j = -\left[\frac{1}{N}\sum_{i=1}^{N}\frac{(\beta_{M_{j,i}}-\beta_{P_{j,i}})^2}{(\beta_{P_{j,1}})^2}\right]^{\frac{1}{2}}, \tag{6}$$

where ε_j represents the quantified error in region j, $\beta_{M_{j,i}}$ is the i-th harmonic component of the curves predicted by the model in region j, and $\beta_{P_{j,i}}$ is the i-th harmonic component corresponding to the measurements taken from the patient in the same region. Therefore, the cost function is defined as follows:

$$F_c = \sum_j \varepsilon_j. \tag{7}$$

2.4 BO and model integration

As described in the introduction, in this work we couple both the Bayesian optimization algorithm and the ADAN86 hemodynamic model to improve the matching between the blood-flow simulation and the available measures of flow and pressure waveforms. For the Bayesian optimization environment, we employ the Python BayesianOptimization library [15], widely used in several optimization tasks [16]. It includes strategies for random sampling of uniformly distributed variables, implementation and optimization of acquisition functions, and the description of the function to be optimized (maximized in this library) as a 'black box' structure. In turn, the ADAN86 model is implemented in C++ and parallelized using MPI. Numerically, the equations are solved using a high-order finite volume method.

After defining the number of initial points to be evaluated for the construction of the initial GP, and the number of iterations to be conducted during the optimization process, the input files for the ADAN86 model are updated with the multiplicative factors corresponding to the parameters to be optimized. The model is then executed as many times as requested by the algorithm as function evaluations. The selected initial points are organized into several folders according to the availability of CPU cores, allowing for parallel execution of the simulations. This approach results in the acquisition of pressure and flow variables across all vascular segments of the ADAN86 model. The segments corresponding to the arterial districts where measurements are available are then selected, and the cost function is calculated. The values of the cost function are stored for each of the evaluated initial points.

After the parallel execution of the initial point groups and the collection of the respective data, we move on to the iteration phase of the Bayesian optimization. At this stage, the process becomes sequential, using the initial points as a foundation for the initial GP construction of the cost function. Based on these points, the algorithm seeks the set of parameters that maximizes the GP of the cost function, continuously refining the estimates with each iteration.

3 Results

To validate the proposed strategy, two virtual patients were synthetically produced from the ADAN86 model. The first one is defined by adapting three parameters: the cross-sectional vessel area (A_0), the elastic modulus of the elastin (E_e), and the arterial wall viscoelasticity factor (γ). As previously commented, the modification of these parameters is addressed by including a multiplicative factor that affects the reference parameter values. For the second synthetic case, the modified parameters were related to the arterial wall mechanics: the elastic modulus of elastin (E_e), the deformation value at which 50% of collagen fibers are recruited (ε_0), and the elastic modulus of collagen fibers (E_c). The multiplicative factors for both synthetic cases are presented in Table 1.

Table 1. Value of the multiplicative factor of the parameters for Virtual Patient 1 and Virtual Patient 2.

Virtual Patient 1			Virtual Patient 2		
A	E_e	γ	E_e	ε_0	E_c
1.35	0.83	2.27	2.1	0.3	1.25

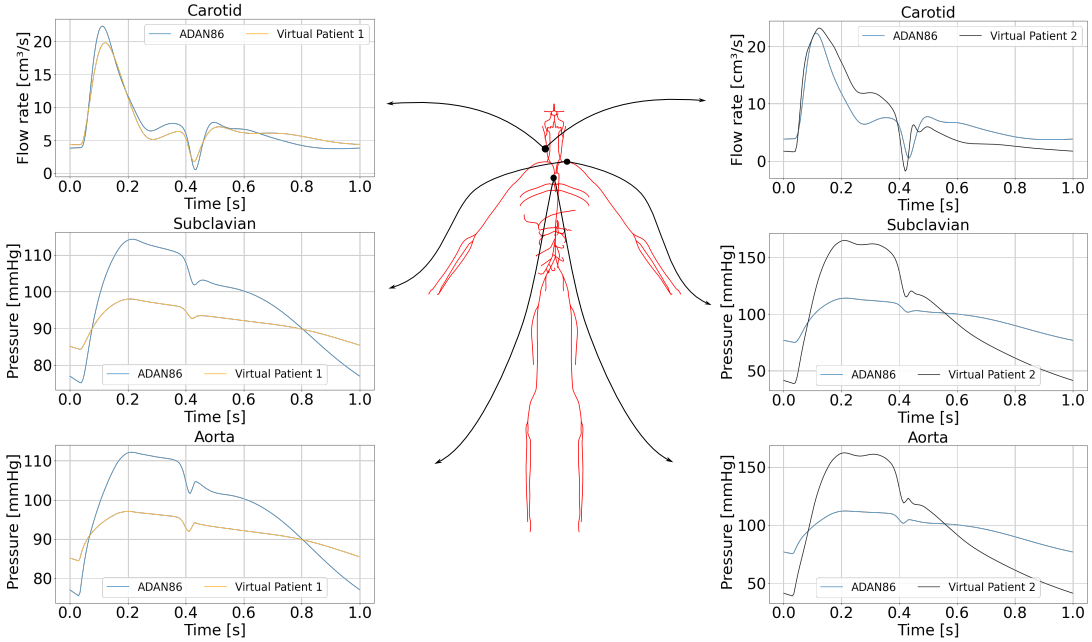

Figure 1. Comparison between the curves predicted by the baseline ADAN86 model (blue) and the synthetic models ADAN1 (orange) and ADAN2 (black). From top to bottom, the comparisons are made for flow rate in the carotid artery, and pressure in the subclavian and ascending aorta arteries.

3.1 Parameter optimization for each patient

In the virtual patient 1, we focused on analyzing the acquisition functions. To evaluate the impact of each function, we used 120 initial points and 100 iterations. We fixed the parameter seed and we use the three available measurements shown on the left panels of Figure 1. We optimized parameters A_0, E_e, and γ as previously described, and the results are represented on the left of Figure 2. Figure 2 illustrates the behavior of the parameters along the iterations. We observed that, for the same number of initial points and iterations, the UCB converged quickly, meaning that the prediction of the ADAN86 model reached the expected value of the virtual patient 1 configurations. In contrast, EI and PoI continued to explore the entire search space, not reaching convergence with this number of conditional iterations for this specific patient. For comparison, we analyzed the curves predicted by the ADAN86 model against the curves of virtual patient 1, as shown on the left of Figure 3. Notably, in the case of

UCB, the curve was identical to that of the virtual patient. However, for EI and PoI, we obtained an optimal value that differed considerably from the patient. Due to the lack of convergence, we demonstrated the random solutions obtained in this interval, which, in the case of pressure, presented a large confidence interval.

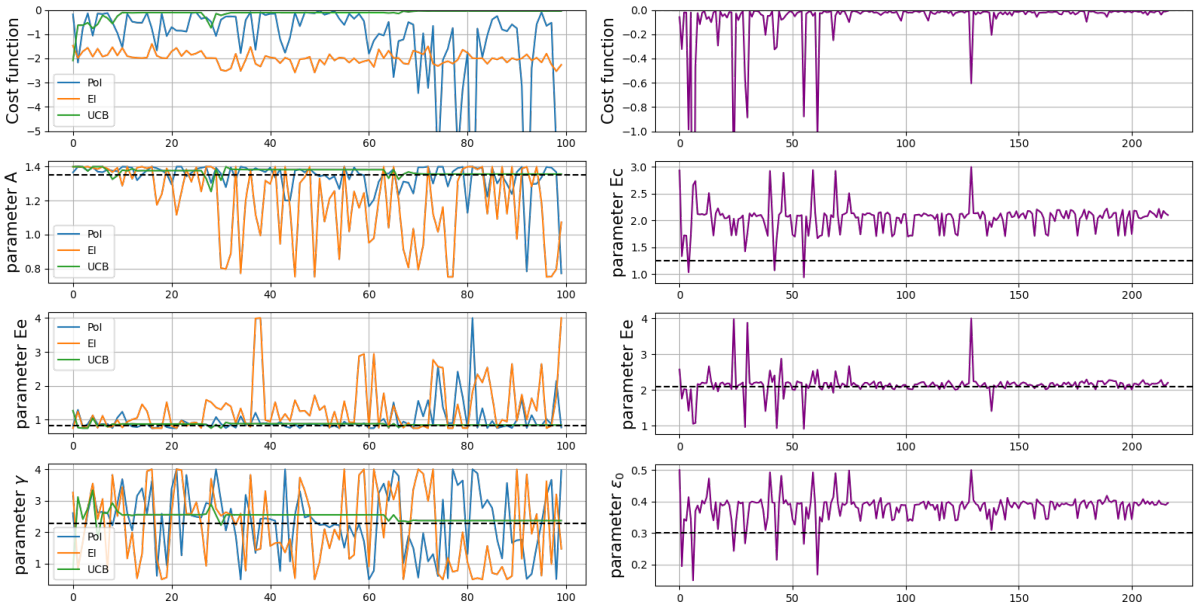

Figure 2. Comparison between the curves predicted by the ADAN86 model (blue) and the synthetic models ADAN1 (orange) and ADAN2 (black). From top to bottom, the comparisons are made for flow in the carotid artery, and pressure in the subclavian and aorta arteries.

In virtual patient 2, we estimated the configurations related to the constitutive response of the arterial wall, specifically E_c, ε_0 and E_e, using 120 initial points and the three available measurements, as represented on the right of Figure 1. The acquisition function used for this patient was UCB, as it demonstrated better performance for virtual patient 1. In this second case, we observed that there was no convergence as seen with UCB in virtual patient 1. The parameters, especially E_e which were very close to each other, did not reach the expected values according to Table 1. Instead, they exhibited variation within a smaller range, particularly the parameters E_c and ε_0. To evaluate the occurrence of these parameters in the curve, we analyzed the graphs on the right of Figure 3. Notably, for the optimal value, the ADAN86 model prediction was the same as the curve of virtual patient 2, and the random solutions exhibited a comparatively smaller confidence interval.

4 Conclusions

We conclude that Bayesian optimization combined with the ADAN86 model were effective at the parameter estimation task, highlighting its potential to capture patient-specific characteristics by proper modification of model parameters. Our findings indicate that parameters such as vessel cross-sectional area (A_0), arterial wall elastic modulus (E_e), and arterial wall viscoelasticity (γ) exert a significantly greater influence on model predictions compared to parameters like ε_0 (the deformation value activating 50% of collagen fibers) and E_c (modulus of elasticity of collagen fibers).

These results offer promising insights for the calibration of model parameters in patient-specific settings, where physiological conditions and data quality from catheterization or ultrasound measurements may be challenging. Bayesian optimization emerges as an advanced tool to perform patient-specific characterization in clinical scenarios. Consequently, future efforts will focus on estimating factors of parameters A_0, E_e, and γ from real patient data, alongside the estimation of cardiac ejection parameters. This combined approach can enhance the calibration capabilities and improve the matching between real-world patient data and model predictions.

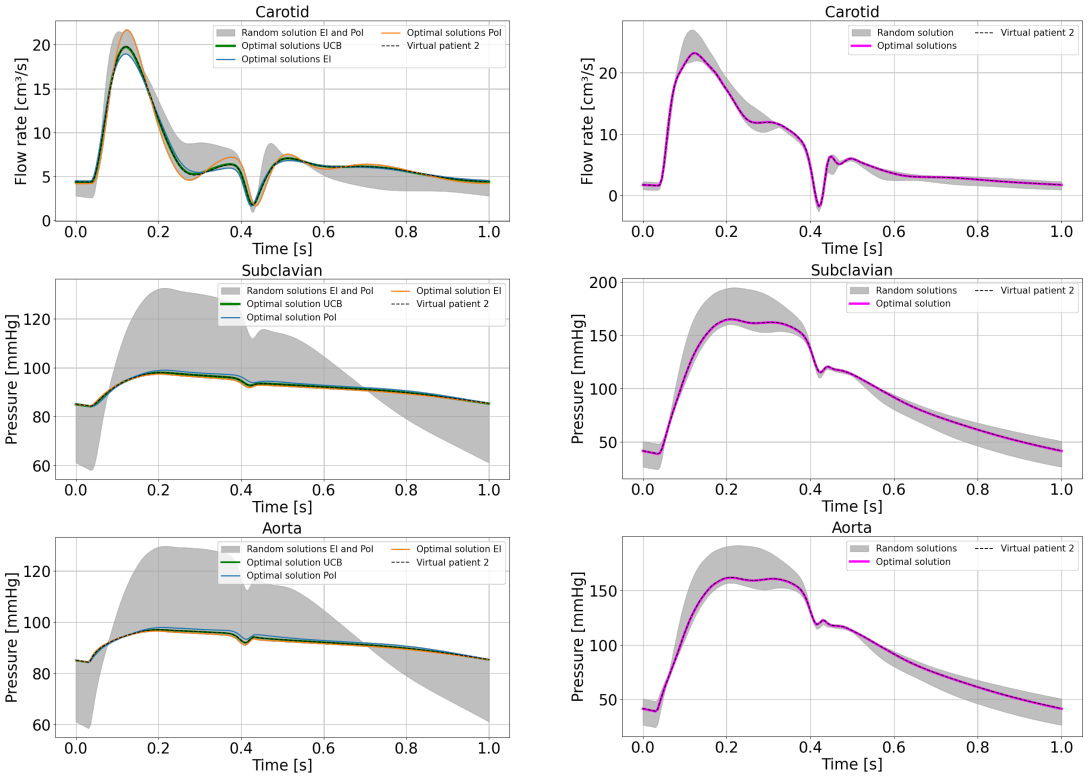

Figure 3. Model ADAN86 predictions for carotid flow and pressure in the subclavian and ascending aorta arteries compared with the curves of virtual patient 1 (on the left) and virtual patient 2 (on the right).

Acknowledgements. I would like to thank the funding agencies CNPq and FAPERJ, as well as LNCC for their continued assistance.

Authorship statement. The authors hereby confirm that they are the sole liable persons responsible for the authorship of this work, and that all material that has been herein included as part of the present paper is either the property (and authorship) of the authors, or has the permission of the owners to be included here.

References

[1] A. L. Colunga, M. J. Colebank, R. Program, and M. S. Olufsen. Parameter inference in a computational model of haemodynamics in pulmonary hypertension. *Journal of the Royal Society Interface*, vol. 20, n. 200, pp. 20220735, 2023.

[2] A. Ü. Coşkun, C. Chen, P. H. Stone, and C. L. Feldman. Computational fluid dynamics tools can be used to predict the progression of coronary artery disease. *Physica A: Statistical Mechanics and its Applications*, vol. 362, n. 1, pp. 182–190, 2006.

[3] R. Botnar, G. Rappitsch, M. B. Scheidegger, D. Liepsch, K. Perktold, and P. Boesiger. Hemodynamics in the carotid artery bifurcation:: a comparison between numerical simulations and in vitro mri measurements. *Journal of biomechanics*, vol. 33, n. 2, pp. 137–144, 2000.

[4] S. Safaei, C. P. Bradley, V. Suresh, K. Mithraratne, A. Muller, H. Ho, D. Ladd, L. R. Hellevik, S. W. Omholt, J. G. Chase, and others. Roadmap for cardiovascular circulation model. *The Journal of physiology*, vol. 594, n. 23, pp. 6909–6928, 2016.

[5] P. J. Blanco, L. O. Müller, S. M. Watanabe, and R. A. Feijóo. On the anatomical definition of arterial networks in blood flow simulations: comparison of detailed and simplified models. *Biomechanics and Modeling in Mechanobiology*, vol. 19, pp. 1663–1678, 2020.

[6] L. Itu, P. Sharma, T. Passerini, A. Kamen, C. Suciu, and D. Comaniciu. A parameter estimation framework for patient-specific hemodynamic computations. *Journal of Computational Physics*, vol. 281, pp. 316–333, 2015.

[7] T. J. Gundert, A. L. Marsden, W. Yang, and J. F. LaDisa Jr. Optimization of Cardiovascular Stent Design Using Computational Fluid Dynamics. *Journal of Biomechanical Engineering*, vol. 134, n. 1, pp. 011002–1–011002–8,

2012.
[8] P. J. Blanco, S. M. Watanabe, E. A. Dari, M. A. R. Passos, and R. A. Feijóo. Blood flow distribution in an anatomically detailed arterial network model: criteria and algorithms. *Biomechanics and modeling in mechanobiology*, vol. 13, pp. 1303–1330, 2014a.
[9] P. J. Blanco, S. M. Watanabe, M. A. R. Passos, P. A. Lemos, and R. A. Feijóo. An anatomically detailed arterial network model for one-dimensional computational hemodynamics. *IEEE Transactions on biomedical engineering*, vol. 62, n. 2, pp. 736–753, 2014b.
[10] P. Blanco, L. Müller, S. Watanabe, and R. Feijóo. Computational modeling of blood flow steal phenomena caused by subclavian stenoses. *Journal of Biomechanics*, vol. 49, n. 9, pp. 1593–1600, 2016.
[11] P. J. Blanco, L. O. Müller, and J. D. Spence. Blood pressure gradients in cerebral arteries: a clue to pathogenesis of cerebral small vessel disease. *Stroke and vascular neurology*, vol. 2, n. 3, 2017.
[12] A. R. Alseiari. *Using Bayesian Optimization Methods in Causal Inference for Sensitivity Analysis*. PhD thesis, McGill University (Canada), 2022.
[13] M. Hoffman, E. Brochu, N. De Freitas, and others. Portfolio allocation for bayesian optimization. In *UAI*, pp. 327–336, 2011.
[14] S. Ranftl, T. S. Müller, U. Windberger, G. Brenn, and von der W. Linden. A bayesian approach to blood rheological uncertainties in aortic hemodynamics. *International Journal for Numerical Methods in Biomedical Engineering*, vol. 39, n. 4, pp. e3576, 2023.
[15] F. Nogueira. Bayesian Optimization: Open source constrained global optimization tool for Python, 2014–.
[16] P. LIU, H. WANG, and W. QIYU. Bayesian optimization with switching cost: Regret analysis and lookahead variants.(2023). In *Proceedings of the 32nd International Joint Conference on Artificial Intelligence, IJCAI*, pp. 19–25, 2023.